ROMANIAN JOURNAL OF INFORMATION SCIENCE AND TECHNOLOGY
Volume **17**, Number 4, 2014, 320–339

Development and Experimental Results on LTCC Packages for Acoustic Wave Sensing Devices

I. GIANGU[(1,2)], V. BUICULESCU[1], F. BECHTOLD[5], G. KONSTANTINIDIS[3], K. SZACIŁOWSKI[4], A. STEFANESCU[1], K. PILARCZYK[4], A. STAVRINIDIS[3], P. KWOLEK[4], G. STAVRINIDIS[3], J. MECH[4], A. MÜLLER[1]

[1] National Institute for Research and Development in Microtechnologies - IMT, 126A (32B) Erou Iancu Nicolae, 077190 Bucharest, Romania
E-mail: ioana.giangu@imt.ro

[2] Faculty of Electronics, Telecommunications and Information Technology, "*Politehnica*" University of Bucharest, Bucharest, Romania

[3] FORTH-IESL-MRG Heraklion, Crete, Greece
E-mail: aek@physics.uoc.gr

[4] Faculty of Non-Ferrous Metals, AGH University of Science and Technology, Al. Mickiewicza 30, 30-059 Kraków, Poland
E-mail: szacilow@agh.edu.pl

[5] VIA electronic GmbH, Robert-Friese-Strasse 3, 07629 Hermsdorf, Germany
E-mail: bechtold@via-electronic.de

Abstract. Novel LTCC packages intended for acoustic wave sensing devices chip assembly are proposed in this paper. A single assembly operation was required for both structure models based on DuPont 9K7 "green" tapes, after layout design and interactive 3-D electromagnetic optimization processes. Due to LTCC manufacturing technology, a large number of package structures containing cavities, inner vertical and horizontal interconnects, pads for inner components' assembly and external signal connections was manufactured. Surfaces acoustic wave (SAW) resonators and film bulk acoustic resonator (FBAR) structures have been used with very good results as temperature and, respectively, humidity sensing devices. Input and output signal ports have been define as coplanar transmission line (CPW) configuration for a good impedance matching to the measuring system. Linear behavior of the frequency shift vs.

temperature and, respectively, relative humidity was evidenced. Although certain temperature sensitivity reduction is observed, an improved dynamic range of the return loss response is noticed for packaged SAW devices, favorable for subsequent signal processing and temperature value extracting. Very small and complex RF packages, with SMT compatible and solderable AgPt pinout and two different levels of Au pads for Au wire bonding inside the cavity intended to provide handling protection after wire bonding are the main outcome of this paper.

Key words: Acoustic wave sensors; Coplanar transmission line; Low temperature co-fired ceramic (LTCC) package; Surface mount assembly.

1. Introduction

Low Temperature Co-fired Ceramic (LTCC) is a complex compound which incorporates glass and ceramic powders, used in multilayer substrates suitable for RF devices packaging due to its very good electrical and mechanical properties [1]. LTCC has become an attractive material system due to its moderate production costs, good heat conductivity [2], high quality factor passive devices and low loss transmission lines for microwave circuits [3]. Moreover LTCC packages use materials with reasonable dielectric constants (ε_r between 4 and 8) offering wider microwave transmission lines, thus leading to lower conductor loss than circuits on Si or other materials[4]. The main advantage of the LTCC ceramic tapes consists in their mechanical processing flexibility, enabling the configuration of complex 3-D structures with channels, membranes, cavities, holes and vertical interconnections between layers using laser or mechanical drilling.

As it is well known the main two components of the LTCC system are the ceramic tape sheets (green tape) and the conductive pastes. For instance DuPont GreenTape 9K7 is a suitable choice for high frequency applications, including wireless and mobile communications [5]. This ceramic tape has stable dielectric properties during multiple re-firing, important for customization of the top or bottom layers for subsequent post-processing, low loss tangent useful for wireless communications and high accuracy in its shrinkage [6].

This technology has a good reliability and stability in harsh environment applications such as high temperature or pressure conditions, [5] providing a hermetic and clean sealing of the RF devices [8] or direct access to the surface assembling techniques[9]. Due to relative *low temperature* (normally not exceeding 1000 $^\circ$ C) used for sintering all dielectric layers and materials typically used for thick-film processing, certain metals with high electrical conductivity and low melting point, such as silver, gold, copper, platinum and palladium [10] can be used. Before stacking and lamination under pressure this metals are screen printed on the un-fired green tape. The multilayer ceramic stack is then sintered [11]. Via holes diameter has to be close to the tape thickness and round catch pads shall be used in order to overlap the via on all sides. By punching the individual tape sheets before lamination (in the unfired state),

cavities or holes can be manufactured according to the design specifications [11].

Integrating embedded passives and manufacturing of RF and microwave transmission or bias lines are easily realized in LTCC technology. The physical and chemical incompatibility of some conductive thick-film materials with LTCC tapes [12] is one of the disadvantages of this technology.

In this paper the surface acoustic wave resonator (SAW) and film bulk acoustic wave resonator (FBAR) have been used as sensing devices. The SAW device's resonance frequency is linear dependent on temperature, since a temperature increase produces a linear expansion of its dimensions and a corresponding change of sound speed in the piezoelectric material. FBARs have been used as humidity sensors and their resonance frequency changes due to mass loading as result of water vapor adsorption.

The quality of wide band gap materials (GaN, AlN) thin layers, grown or deposited on SiC, sapphire and also on Si substrate, improved a lot in the last years. GaN and AlN have good piezoelectric properties but only recently they could be used for SAW and FBAR devices manufacturing. These materials can be used to increase the resonance frequency of acoustic devices using advanced micromachining and nanoprocessing technologies. An increased resonant frequency has as effect a higher sensitivity of the device; the sensitivity is proportional with the resonance frequency for temperature and pressure sensors and with the square of the resonance frequency for chemical and humidity sensors [14]. SAW devices with resonance frequencies higher than 5 GHz on GaN/Si [15] and AlN/Si [16] have been manufactured. Also FBAR devices on GaN have been fabricated [17]–[20]. First results regarding humidity sensors on GaN were reported in [21].

Considering the fact that, for this type of sensing devices, no LTCC package has been reported in literature so far, we proposed for the first time two specifically designed and manufactured LTCC packages with different layouts for SAW respectively FBAR sensing devices packaging. All simulation and optimization results presented in this paper are exclusively based on 3-D electromagnetic analysis software CST Microwave Studio [22].

2. Design requirements and concept

Since it was demonstrated that the single-port SAW devices are more sensitive than those with two ports or delay line [14], single SAW resonators with resonance frequencies higher than 5 GHz on GaN/Si [15] have been used as temperature sensors. The reflection coefficient and its corresponding input impedance are the only measurable parameters of these sensors. FBAR devices manufactured on a 0.5 μm thin GaN membrane and 50 nm Mo metallization have been used as humidity sensors, based on design and the technological processes developed in [17]. They are two-port structures, hence for microwave characterization the complete parameter set *i.e.* [Z] or [Y] for lower RF frequency range, whereas [S] parameters are used in the upper frequency range.

A major advantage of LTCC packaging results from the possibility to integrate in a single structure a large number of passive components with complex inter-connections, especially for direct current bias lines and low frequency circuits, resulting from multiple layers' availability. Inductive and capacitive parasitic elements associated to the LTCC packages should have very low reactance in order to reduce their impedance transforming action observed at the packages' external terminals or connecting pads. This is usually true for packages with (very) small dimensions, or less influenced by transmission line (TL) type structures, specific only to the larger configurations. As the working frequency increases, specific rules must be applied in order to maintain a good impedance matching between stages, use of transmission lines for RF connections and very low power losses. The last condition requires satisfying design conditions related to parasitic coupling minimizing over the whole package, and a layout design based on efficient shielding as well.

High frequency components or monolithic integrated circuits can be also incorporated in LTCC packages by mounting them by means of coplanar or microstrip transmission lines, located on accessible layers after the complete package manufacturing process is finished. The transmission of the signal through vertical metal filled via holes leads to a reduced volume of the LTCC component, but the system must have a low height so that the equivalent inductance of the metalized holes to be reduced [22].

According to the aspects mentioned above, both packages proposed in this paper have structures made of the same number of layers, open cavities for both chip assembly and direct environmental condition sensing, and vertical metal filled via holes (VMFH) for connecting the internal signal and ground pads to the corresponding external pads. The main differences between these two LTCC packages consist in (i) their layout related to the required signal ports and (ii) electrical specifications. For instance, only two external connection pads are necessary for the single-port SAW structure, whereas two pairs of coplanar type transmission lines (CPW) have to be provided for the input and output signals in case of two-port FBAR devices. Therefore, in the LTCC package design process we have to take into account the number of each device's number of ports and the minimization of the costs by unifying the technological processes.

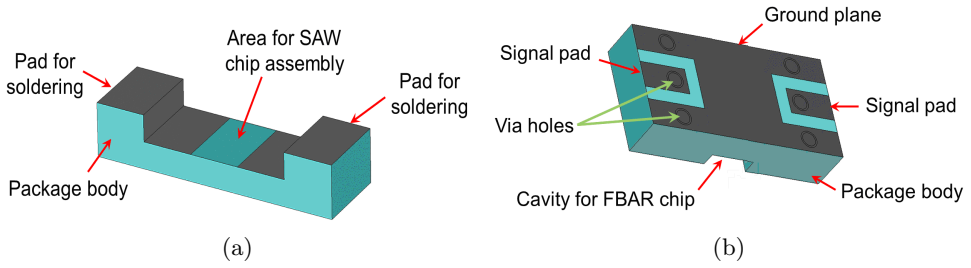

Fig. 1. The concept LTCC package for: (a) SAW structure (front view) and (b) FBAR structure (bottom view).

The concept presented in Fig. 1a for a SAW package is provided with two large pads entering a cavity for device connection with gold wires. The FBAR package (Fig. 1b) is provided with two sets of CPW type pads for input and output signals on the backside. The connection to the ground plane is distributed over the remaining area, taking into account the general rules for the design of CPW lines, which refers to the signal line widths and the corresponding gaps separating the signal line from a pair of ground planes located symmetrically from it in most cases. Metalized holes connect each internal pad to the corresponding external pad because of different plane positioning of these pads. If technological constraints and available package dimensions allow, more holes can be used for each vertical connection, with the advantage of equivalent inductance reduction.

3. LTCC packages – Design Preview

The acoustic wave resonators are in the form of rectangular structures (Fig. 2), with areas of about 0.8 mm^2 (SAW) and, respectively, 1.9 mm^2 (FBAR). Each device is provided with pads placed on the top side of the chip, fully compatible with the CPW probes of the vector network analyzer (VNA) model 37397D from Anritsu, with contact fingers placed at 150 μm distance.

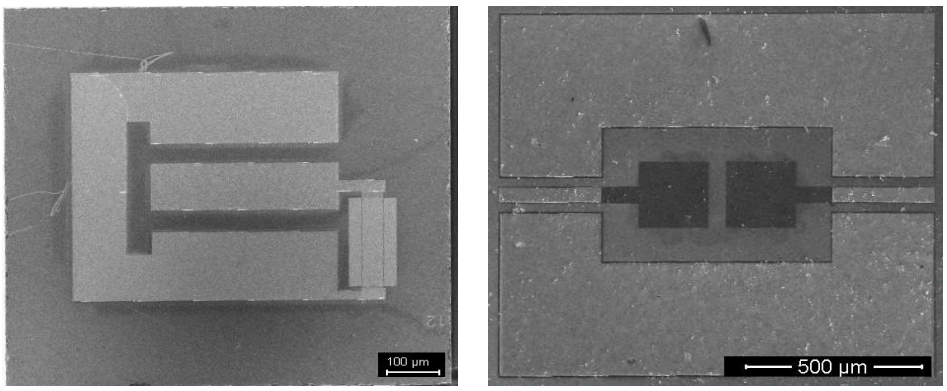

(a) (b)

Fig. 2. SAW [15] and FBAR [17] chips before packaging.

Two LTCC package models using the same stacked structure were developed for these acoustic wave devices, with specific differences only in dimensions and pad arrangement. Table 1 summarizes the technical and technological parameters used for assessing the preliminary mechanical design of the LTCC packages, according to manufacturer's requirements and specific sensing applications with SAW and FBAR structures.

The electrical design of both packages is subject to some material properties directly related to ceramic material chosen for manufacturing: (i) relative dielectric permittivity and (ii) LTCC tape shrinkage in horizontal plane and vertical direction.

Their values should be the "final" ones – from the beginning of 3-D simulation to the last mechanical design steps – hence they are considered after firing process, in order to maintain the parameter correctness of the manufactured products.

Table 1. Main material and technological characteristics

No.	Characteristic	Value	Unit
1.	Ceramic material	DuPont 9K7	–
2.	Relative permittivity	7.1	–
3.	Loss tangent	0.001	–
4.	Sheet thickness ("green" tape – see the note)	254 ± 14	μm
5.	Number of layers	6	–
6.	X/Y (horizontal) shrinkage	9.1 ± 0.3	%
7.	Z (vertical) shrinkage	11.8 ± 0.5	%
8.	SAW chip dimensions (L × W × H)	920 × 850 × 500	μm
9.	FBAR chip dimensions (L × W × H)	2000 × 1800 × 100	μm

Note: "Green" tape term means tape before final thermal processing.

The "green" tape thickness of 254 μm and the number of six layers, common for both packages, were chosen in such a way as to be satisfied all assembly and mechanical strength conditions, including relative permittivity of the substrate *after* firing and ceramic substrate shrinking during high temperature processes. Final mechanical design takes into account all other mechanical limits existing in relevant documents available from the package manufacturer [23] and presented in Table 2.

Table 2. In-house dimensions and tolerances of some LTCC technological elements [23]

No.	Characteristic	Value (*sintered*)	Unit
1.	Usable green sheet dimensions	145 × 145	mm
2.	Via hole diameter	≥ 175	μm
3.	Via spacing	≥175	μm
4.	Via center to part edge	≥475	μm
5.	Stacked vias (maximum)	3	–
6.	Punching tolerance	±10	μm
7.	Tape layer stability	±35	μm
8.	Alignment pattern to via/pattern	±25	μm
9.	Alignment layer to layer	±35	μm
10.	Cavity floor thickness	≥400	μm
11.	Cavity depth	≤ 800	μm
12.	Corner radius	≥ 250	μm

Note: Characteristics above are typical, excepting special marking.

First approach result (Fig. 3) shows the ordered sequence of layers associated to the SAW package and their specific layout elements: pads for SMD assembly of the package (external) or SAW connections (inner) with thin Au wires, plated vertical via holes for signal connections, and windows or cuttings of different dimensions required

for chip insertion and access for wire bonding. There are two bottom sheets provided exclusively for supporting the SAW chip and external connection pads, as an optimum choice between manufacturing cost (it asks for a minimum number of layers) and reliability, determined by the proper number of layers, at least two for 254 μm tape thickness used in our design.

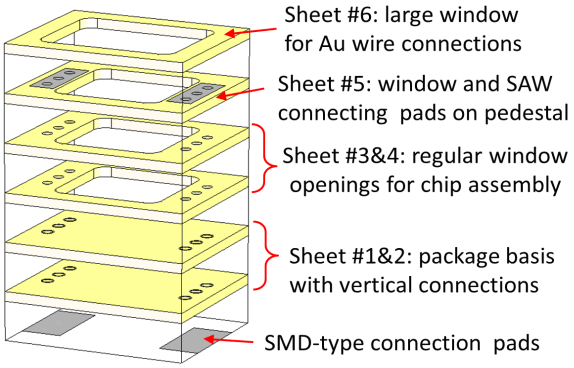

Fig. 3. Simplified LTCC package layout used for SAW sensor assembly.

3.1. LTCC and multi-layer connections

Circuit layout design for complex LTCC components requires a special attention to the *vertical* structure development, mainly for inter-layer connection rules and limitations. The first step considers an unitary procedure used to build a vertical connection between stacked layers taking into account that:

- a single vertical connection may pass any number of layers (or tapes), depending only on package's complexity;
- all via holes used for these connections are processed with a limited accuracy;
- stack assembly can be also a source of random, small missalignments between adjacent holes used in the same connection, although a certain offset is sometimes desired, in order to avoid geometrical distortions during later technological stages;
- the conductive pastes used to fill the via holes have a certain viscosity, hence they can flow through a single layer only [25];
- pad and conductor printing follows after via filling.

As a result, a "mushroom-like" structure (Fig. 4a) has to be defined around each via intended for a vertical connection, and upon each tape of the stacked connection. This way, each via hole is filled with conductive paste and integrated with its surrounding pad (defined in a subsequent step by depositing a conductive paste through

a silk screen), as required to compensate for small errors due to drilling the holes or tape alignment mentioned above (an example is presented in Fig. 4b).

The next step consists in stacking all tapes forming part from the package, as shown in Fig. 4c, where the individual metal-plated structures are only made visible (some distance between is still kept) while the "green" tapes are completely hidden for the sake of clarity. Finally, the completely assembled structure enters the hot isostatic pressing stage, thus enabling the diffusion bonding of all deposited metallic layers in direct mechanical contact and formation of continuous signal connections.

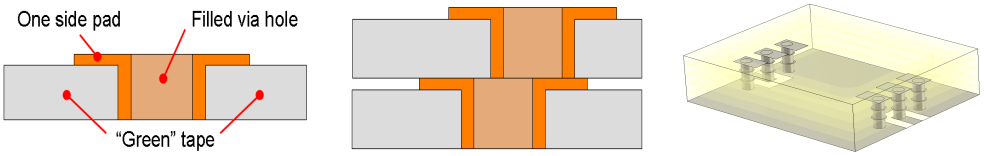

Fig. 3. Technological steps for multi-layer assembly: via hole filling and pad plating (a); via hole misalignment during layer stacking – not to scale (b); example of pad connections through three layers, with translucent LTCC tapes (c).

3.2. SAW package

The SAW resonator is a one-port device, hence it needs two pads only for full connection in a RF circuit. The corresponding package (Fig. 5) has metal plated pads, vertical via holes (also metal filled) and cavities for chip protection and assembly specifically defined for each layer. Two wide pads placed inside of package's cavity are used to connect locally the SAW structure with gold wires. Further connections to the bottom pads are obtained through three metal plated via holes for each pad, in order to decrease their total equivalent inductance.

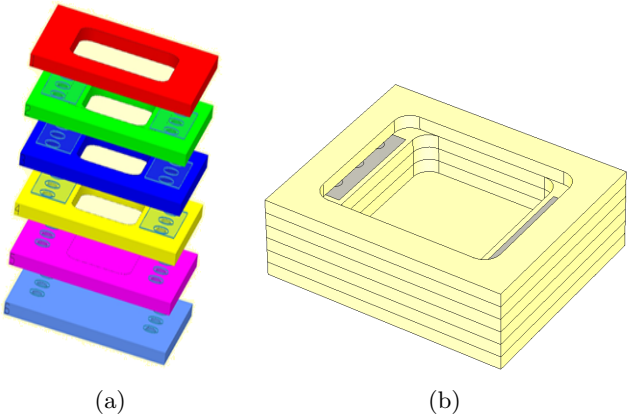

Fig. 5. LTCC package proposed for SAW resonators: exploded views (a) and after assembly (b).

3.3. FBAR package

The package model for an FBAR device is presented in Fig. 6. The main structural difference from previous component consists in number and placement of signal and ground pads, because the FBAR is a two-port component. As a result, the bottom metal structure for signal input and output has two CPW pads, while the ground metal layer fills the rest of the bottom area, taking into account the specific design rules, regarding line widths and corresponding gaps. In addition, the filter behaviour requires controlled characteristic impedance along metal structure starting from bottom CPW interface up to the top (inner) pads used for BFAR connection with Au wires.

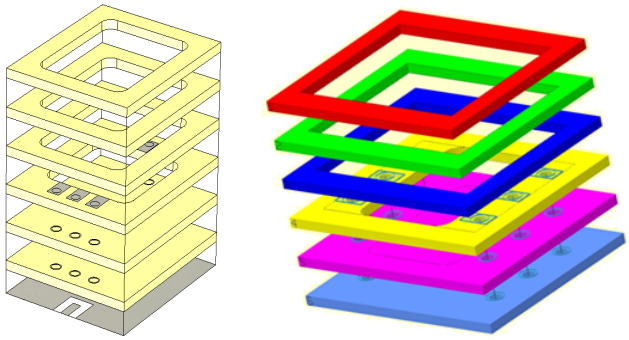

(a) (b)

Fig. 6. Exploded views of the FBAR LTCC package: preliminary design (a) and according to prototype file (b).

4. Analysis of the LTCC package for SAW sensors

Figure 7a presents the structure used for 3-D electromagnetic simulation of the complete package. The LTCC package is represented by (i) inner elements (via holes and inter-layer pads), (ii) external pads placed on the bottom side of the package (not visible in figure), (iii) internal pads required for connecting the SAW resonator and (iv) a single gold wire replacing the equal-length pair of SAW connections.
The simulation results shown in Fig. 7b correspond to the package's input impedance calculated at the level of external connection pads, placed on bottom package side and used for soldering of the packaged SAW as surface mounted device (SMD). The impedances corresponding to each of the three frequency markers (0.5 GHz, 5.5 GHz and 8 GHz) are presented in Table 3.

Table 3. Impedance values vs. simulation frequency

Frequency	**Re** $(\boldsymbol{Z}_{in})$ [Ω]	**Im** $(\boldsymbol{Z}_{in})$ [Ω]
$f_L = 0.5$ GHz	0.0473	6.310
$f_M = 5.5$ GHz	7.984	80.74
$f_H = 8.0$ GHz	30.4	142

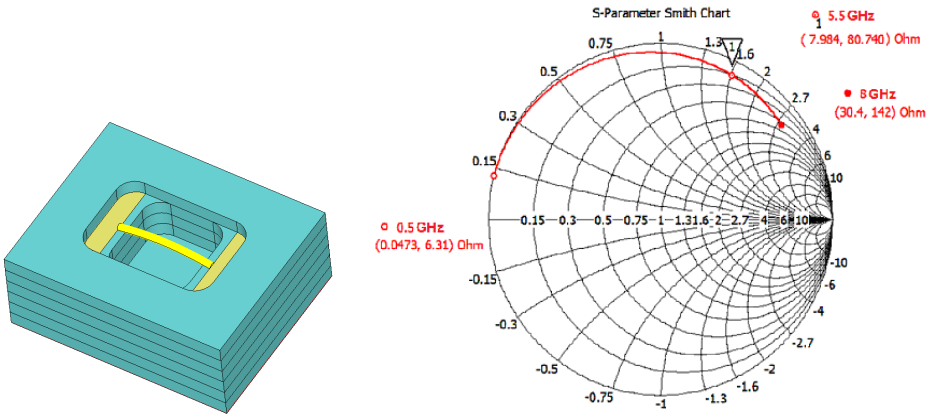

(a) (b)

Fig. 7. Effect of Au wire on LTCC package: (a) structure; (b) simulated results.

These impedances can be used to obtain the component values for each equivalent circuit's model with discrete components shown in Fig. 8 and, consequently, validation of the best one.

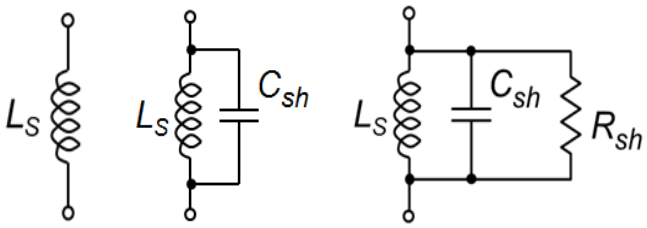

(a) (b) (c)

Fig. 8. Discrete models associated to the simulated result in Fig. 7: inductor (a); shunt LC (b); complete, lossy (c).

The first step consists in analyzing the simplest available structure (Fig. 8a). Considering that package's inductive reactance at the lowest simulation frequency ($f_L = 0.5$ GHz) is not affected by additional reactances due to other structural elements, then

$$L_s = \frac{Im(Z_{in}@f_L)}{\omega_L}. \tag{1}$$

Solving (1) at frequency f_L, the series inductance is $L_S = 2.0085$ nH. If the reactance of this inductor is calculated at other frequency f (e.g. $f = f_M$ or $f = f_H$), a relative error e_R can be calculated from the measured reactance (according to Table 3) as:

$$e_R(f) = \frac{Im[Z_{in}(f)] - X_{calc}(f)}{Im[Z_{in}(f)]}, \tag{2}$$

where $X_{calc}(f)$ is the reactance calculated at the terminals of corresponding component shown in Fig. 8.

The results for single inductor model are presented in Table 4 (row marked **M1**).

Table 4. Calculated errors for different package models

Model number	Model description	Calculated error @ frequency		
		0.5 GHz	**5.5 GHz**	**8 GHz**
M1	Fig. 8a	0 %	–14 %	–28.9 %
M2	Fig. 8b	–0.12 %	0 %	1.12 %

The next step considers the second model (Fig. 8b), with a capacitor C_{sh} in shunt connection with L_S for compensating, to a certain extent, the errors due to single inductor model. The same inductor value is used as in the previous step, but the shunt capacitor's value is obtained from the condition to have the same reactance at frequency f_M:

$$\frac{1}{Im(Z_{in}@f_M)} = \frac{1}{\omega_M L_S} - \omega_M C_{sh}. \tag{3}$$

The result is $C_{sh} = 0.05851$ pF, therefore corresponding error terms in the row marked **M2** of Table 4 can be calculated. The new errors, e.g. 1.12% at f_M, are much lower compared with previous values for the single inductor model and completely satisfactory for the simulation stage.

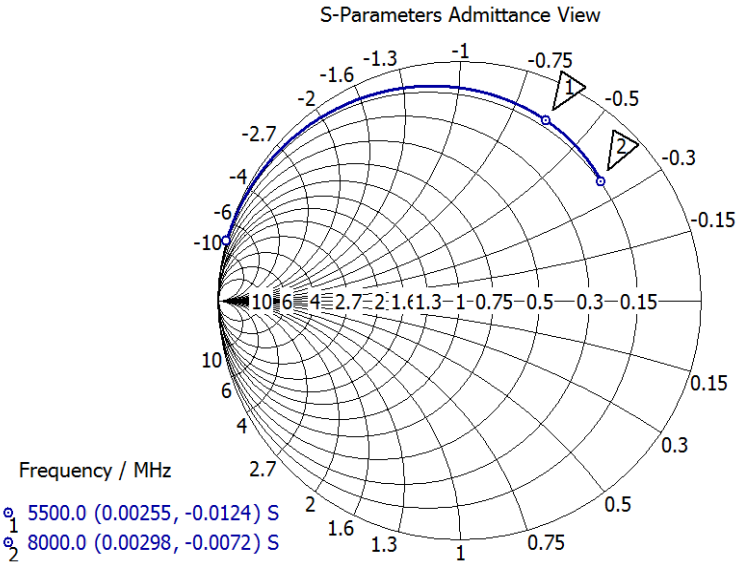

Fig. 9. Procedure for extraction of R_{sh}.

The final step consists in calculation of the shunt resistor R_{sh}, after replacing the previously obtained values. This can be performed after the impedance graph

shown in Fig. 7b is translated on *admitance* Smith chart (Fig. 9). In this case, the admitance graph follows approximately a constant conductance circle; R_{sh} values can be calculated for each marker frequency from:

$$R_{sh} = 1/G. \tag{4}$$

The corresponding conductances represented in Fig. 9 are G_1 (5.5 GHz) = 0.00255 S (Marker1) and G_2 (8 GHz) = 0.00298 S (Marker2), respectively, therefore R_{sh1} = 392.2 Ω and R_{sh2} = 335.6 Ω.

Although the ratio of these values is about 1.17, i.e. a difference of 17% between resistances, the result is considered acceptable with the actual package, because (i) the actual dielectric loss is extremely small (according to Table 1), and PEC (Perfectly Electric Conducting) materials are defined for metallic structures like pads and connection elements. From technological point of view, this statement is supported by high quality conductive pastes used for all these elements, while their small dimensions do not justify these losses.

Figure 10 presents the simulation of packaging effect on input impedance of a SAW chip initially measured on wafer, using scalar (return loss) and vector (Smith chart) representations. Both L_S and C_{sh} values calculated above are used for this simulation. Although not shown explicitly, the shunt resistor has insignificant influence on either representation of the SAW behaviour, due to the high ratio (more than six times) compared with regular 50 Ω generator impedance of the network analyzer.

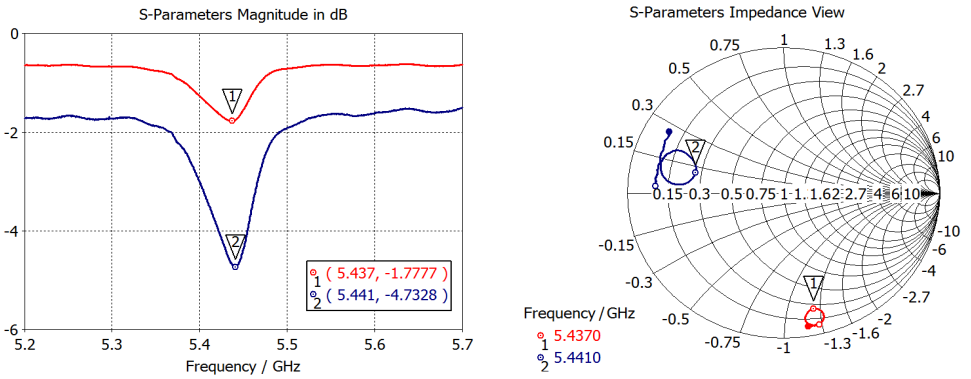

(a) (b)

Fig. 10. Return loss (a) and Smith chart (b) simulations of SAW behaviour after packaging.

It is noticed an improvement in amplitude of the return loss minimum in case of packaged SAW (marker#2), compared with on-wafer measurement (marker#1). This result is important for temperature measurements, because the dynamic range increase that corresponds to the return loss amplitude changes is easier processed. At the same time, a small frequency shift is observed for the frequency associated to a response minimum (ratio of marker#1 to marker #2 frequencies). This in not

an inconvenient, because each SAW sensor is accurately calibrated *a priori* within actual temperature measurement set-up. Besides, the relative frequency shift due to parasitic elements of the package is less than 1% and, since it is expected to remain almost constant, the effect on sensor's sensitivity [25] remains negligible. However, it is expected that the SAW response described above is somewhat distorted by these reactive elements, especially due to its resonant behaviour.

5. Analysis and optimization of the LTCC package for FBAR sensors

Both design and technological rules mentioned above and related to the SAW resonator package remain also valid for the FBAR package model. For this reason, the main dimensions of generic internal metallic structure shown in Fig. 11, *i.e.* via hole diameters and distances between them were optimized in order to obtain reduced return loss on each outer port of the package. However, the dimensions of each structural element type has to comply with mandatory technological limits shown in Table 2, regardless of the degree of achievement of electrical optimization requirements.

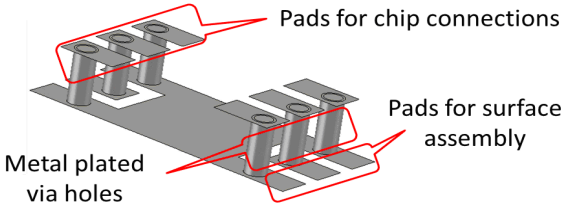

Fig. 11. Simplified metallic structure of the LTCC package for FBAR devices.

Three transmission environment levels are observed in this figure:

1. regular CPW on the bottom side, intended as external pads for standard surface assembling of the package;
2. GSG (ground-signal-ground) trifilar transmission line - with cylinder-like conductors (metal plated via holes), of which two are for grounding - used for vertical connections,
3. CPW-like transmission line (GSG) on an elevated plane, used as internal pads for the FBAR chip connections.

Since these short transmission line sections are cascaded, their **assembly** has to perform as a single transmission line of controlled characteristic impedance $Z_0 = 50\ \Omega$.

Discrete (multi-pin) ports were added at the external and internal pad interfaces, as presented in Fig. 12a, because the package structure's complexity and the spatial development – with input and output elements for signal access located in different, perpendicular planes – did not allow the convenient use of regular waveguide type ports.

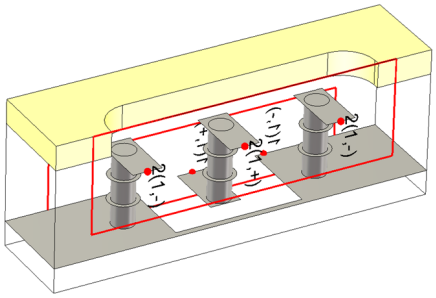

(a)

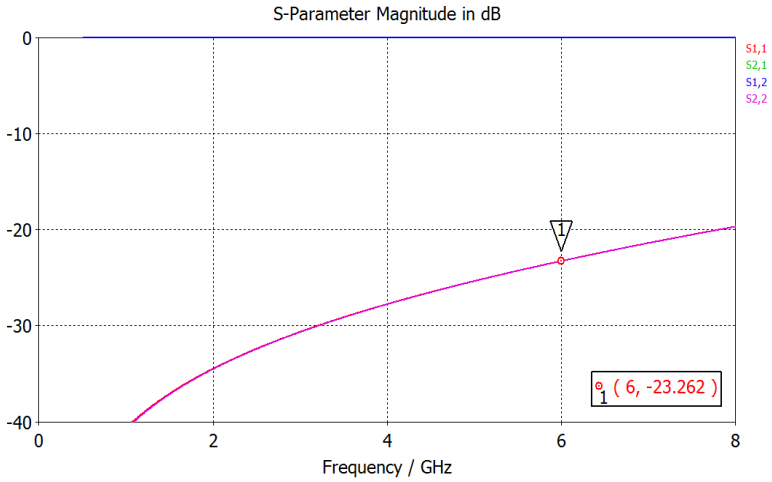

(b)

Fig. 12. RF analysis of CPW port of the FBAR connection: (a) definition of discrete ports; (b) simulated S-parameters – transmission and input/output matching.

The optimization task was set to adjust more variables for minimizing the return loss of equivalent transmission line that describes the broadband behaviour of complete structure:

- distance between metal plated via holes and their diameter, taking into account the minimum available distance between bottom pads;
- distances from the signal pad, on bottom plane, to the surrounding ground area;
- width and length of all GSG pads located upon elevated plane.

Although actual FBAR devices cover a frequency range up to 6 GHz, the optimization process was stopped after the return loss decreased below –20 dB at 8 GHz (Fig. 12b), a value higher than the actual one [27]. This frequency limit is considered suitable even for future development of the FBAR structures. On the other

hand, obvious technological constraints on metal structure positioning and dimensions (layout) mentioned above do not allow a further improvement of the package within existing configuration that is specifically designed for full compatibility with the SAW resonator.

6. Technological aspects and experimental results

Concerning technology and manufacturing of LTCC package models described in previous sections, the main challenge has been related to realization of two bonding levels and, at the same time, the use of a low cost, mixed metal system, with compositions and physical-chemical properties related to their specific function: (i) inner pad definition, (ii) via filling, and (iii) external pad printing. From this point of view, we can report probably the first low-cost mixed metal technology RF package on DuPont 9K7 commercial LTCC tape in Europe. Realization of two different packaging designs on a single wafer (multi-wafer approach) was therefore successful.

On July 1^{st}, 2006 the European Union (EU) Waste Electrical and Electronic Equipment Directive (WEEE) and Restriction of Hazardous Substances Directive (RoHS) came into effect prohibiting the inclusion of significant quantities of lead in most consumer electronics produced in the EU; some related regulatory documents and updates, including REACH (Registration, Evaluation, Authorization and Restriction of Chemicals) conformity are detailed in [28]–[30]. Lead-free solders in commercial use may contain tin, copper, silver, bismuth, indium, zinc, antimony, and traces of other metals. Most lead-free replacements for conventional Sn60/Pb40 and Sn63/Pb37 solders have melting points about 5 to 20°C higher compared with lead based ones [11], although solders with much lower melting points are available. Therefore, a special effort was associated to the EU requirements for reducing the use of environment aggressive substances during present package process development.

The result consists in fabrication of very small and complex RF packages with conductive layers adapted to each local technological requirement, and fully SMT compatible external pads. Gold based inner pads are used for SAW and FBAR connections, due to the best compatibility with Au wire bonding. Other compositions are: (i) AgAu paste for via hole filling, resulting from their flow properties and proper viscosity, (ii) AgPd conductive paste for external pads printing – SAC (Sn-Ag-Cu based alloy) soldering, and (iii) Ag paste for the internal "wiring". All these materials are fully REACH and RoHS compliant.

LTCC packages customized for each of the two acoustic sensing devices are shown in Fig. 13. They were assembled on test circuits provided with CPW transmission lines appropriate for specific package models and SMA connectors at the test ports for complete characterization of the SAW and FBAR resonators.

For the packaged SAW structures the dependence of the resonance frequency on temperature shift was determined using reflection parameter (S11) measurements, within 20°C – 140°C temperature range, with a cryostat (SHI-4H-1 from Janis Research Company). The variation of the resonance frequency with temperature can be linearly approximated (Fig. 14). The slope of the corresponding graph represents

device's sensitivity defined as an absolute value [14]:

$$S = \frac{df}{dT}, \tag{5}$$

or, after normalization to the measuring frequency f

$$s = \frac{1}{f} \cdot \frac{df}{dT}, \tag{6}$$

where df is the frequency shift due to temperature change dT.

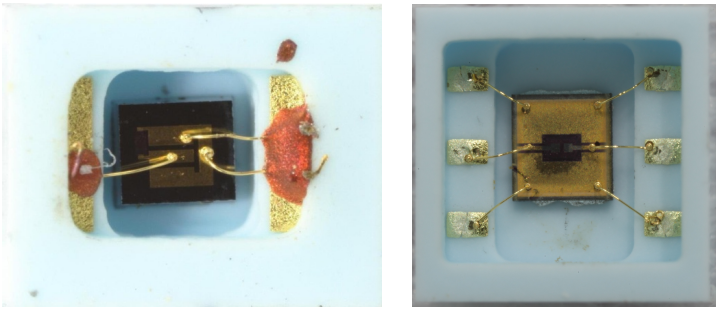

(a) (b)

Fig. 13. LTCC packages with assembled SAW (a) and FBAR (b) structures.

A side effect of the SAW structure packaging consists in its sensitivity decrease comparing with the on-wafer measurements, as evidenced in Fig. 14 [31]. It is mainly attributed to a lower thermal expansion coefficient of the LTCC package compared with on-wafer (*i.e.* mechanically unbounded) SAW chip measurements.

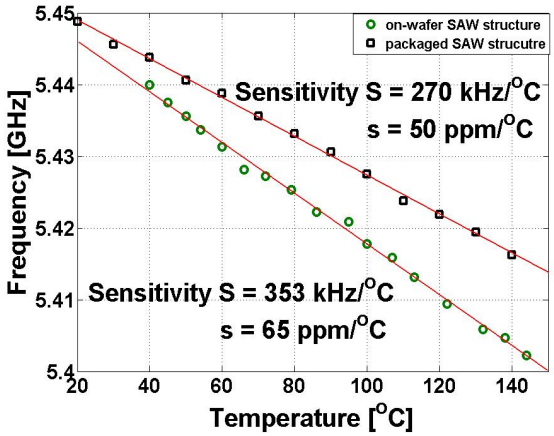

Fig. 14. LTCC packaging effect on SAW sensor sensitivity.

FBAR structures have been coated with a thin layer of a specially designed polymer intended to adsorb only water vapors from the atmosphere (adsorption selectivity). Three polymers were fabricated from a blend of water-soluble polymer and titanium dioxide nanoparticles. The best performance was achieved with materials containing polyvinyl alcohol and nanoparticles with wide diameter distribution ranging from 80 to 1000 nm. The packaged FBAR structures were placed inside of a hermetically sealed small enclosure with controlled humidity.

Fig. 15. Details of the experimental set-up.

Transmission parameter S21 measurements were performed using the VNA. The experimental system used is shown in Fig. 15. The resonance frequency was determined for several values of relative humidity (RH): 1%, 20%, 46%, 66% and 90%. The variation of the resonant frequency with RH is shown in Fig. 16. It can be observed that resonance frequency variation is linear with relative humidity, hence the sensor's sensitivity can be determined from the slope of the characteristic response.

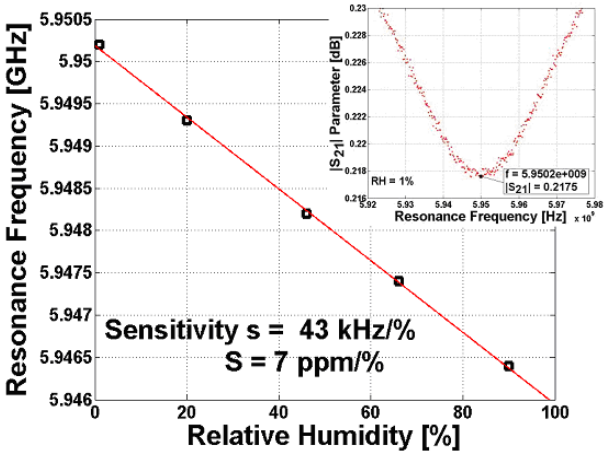

Fig. 16. Resonance frequency vs. RH. The inset represents the resonance frequency at 1% RH.

7. Conclusions

Two novel packages based on LTCC technology have been designed and manufactured for acoustic wave sensing devices. The SAW and FBAR structures were used as temperature and humidity sensing devices. A common six layers stacked structure has been chosen in order to unify the technological processes for both LTCC packages, so minimizing the manufacturing costs. Each layer is a ceramic DuPont 9K7 "green" tape composite with very stable properties. A 3-D electromagnetic simulation of the complete LTCC package for SAW sensor was done in order to determine the package's input impedance. These impedances have been used to obtain the values for the discrete components of the packaged SAW structure equivalent circuit. Simulations of packaging effect on input impedance of the SAW have shown an improvement in amplitude of the return loss minimum and a small resonance frequency shift. In the case of the FBAR structure dimensions of the packages were optimized meeting the RF requirements related to minimum reactive parasitic elements and impedance matching in a broad frequency range. All simulations and optimization process have been realized with CST software. Low cost mixed metal system used as conductive paste and ceramic tapes, both fully REACH and RoHS compatible were used in some technological processes specifically developed for the LTCC packages.

Acknowledgment. The author acknowledge the support of Romanian Authority for Scientific Research, CNCS – UEFISCDI under the project PN-II_PCE-2011-3-0513, program 'Ideas'. The author Ioana Giangu acknowledges also the support of the Sectoral Operational Programme Human Resources Development 2007-2013 of the Ministry of European Funds through the Financial Agreement POSDRU/159/1.5/S/132397.

References

[1] PONCHAK G. E., CHUN D., YOOK J.-G., KATEHI L. P. B., *The Use of Metal Filled Via Holes for Improving Isolation in LTCC RF and Wireless Multichip Packages*, IEEE Transactions on Advanced Packaging, vol. **23**, pp. 88–99, 2000.

[2] MULLER R., WOLLENSCHLAGER F., SCHULZ A., ELKHOULY M., TRAUTWEIN U., HEIN M. A., MULLER J., GARCIA ARIZA A. P., THOMA R. S., *60 GHz Ultrawideband Front-Ends with Gain Control, Phase Shifter, and Wave Guide Transition in LTCC Technology*, IEEE European Conference on Antennas and Propagation (EUCAP), pp. 3255–3259, 2011.

[3] WANG Z., LI P., XU R., LIN W., *A Compact X-Band Receiver Front-End Module Based on Low Temperature Co-fired Ceramic Technology*, Progress In Electromagnetics Research, vol. **92**, pp. 167–180, 2009.

[4] GOLONOKA L. J., *Technology and applications of Low Temperature Cofired Ceramic (LTCC) based sensors and microsystems*, Bulletin of the Polish Academy of Sciences, Technical Sciences, vol. **54**, no. 2, pp. 221–231, 2006.

[5] ROVENSKY T., PIETRIKOVA A., RUMAN K., VEHEC I., *Stability of LTCC Substrates in High Frequency Area After Accelerated Aging Tests*, IEEE Proceedings of the

International Spring Seminar on Electronics Technology (ISSE), vol. **37**, pp. 221–224, 2014.

[6] HANZAZ A. A., *LTCC System for High Frequency Applications*, Proceedings of the International MultiConference of Engineers and Computer Scientists IMECS, vol. **2**, pp. 1055–1058, 2012.

[7] NOWAK D., DZIEDZIC A., *LTCC Package for High Temperature Applications*, Microelectronics Reliability, vol. **51**, pp. 1241–1244, 2011.

[8] LENKKERI J., JUNTUNEN E., LAHTI M., BOUWSTRA S., *Thermo-mechanical Simulations of LTCC packages for RF MEMS Applications*, IEEE International Conference on Thermal. Mechanical and Multiphysics Simulation and Experiments in Micro-Electronics and Micro-Systems, EuroSimE 2010, vol. **1**, pp. 1–6, 2010.

[9] JANTUNEN H., *A novel low temperature cofiring ceramic (LTCC) material for telecommunication devices*, Phd Thesis, University of Oulu, Department of Electrical Engineering and Infotech Oulu, 2001.

[10] FOURNIER Y., *3D Structuration Techniques of LTCC for Microsystems Applications*, Phd Thesis, École Polytechnique Fédérale De Lausanne, 2010.

[11] WOLFF I., *From Antennas to Microwave Systems - LTCC as an Integration Technology for Space Applications*, Proceedings of the 3rd European Conference on Antennas and Propagation, pp. 3–8, 2008.

[12] *** *Design Guidelines Low Temperature Co-fired Ceramic Modules*, VTT Electronics, Version 1.3

[13] BIROL H., MAEDER T., NADZEYKA I., BOERS M., RYSER P., *Fabrication of a millinewton force sensor using low temperature co-fired ceramic (LTCC) technology*, Sensors and Actuators A: Physical, vol. 134, pp. 334–338, 2007.

[14] MÜLLER A. et al, *GaN/Si based single SAW resonator temperature sensor operating in the GHz frequency range*, Sensors and Actuators A: Physical, vol. **209**, pp. 115–123, March 2014.

[15] MÜLLER A., NECULOIU D. et al, *SAW devices manufactured on GaN/Si for frequencies beyond 5 GHz*, IEEE Electron Devices Letters, vol. **31**, no. 12, pp. 1398–1400, 2010.

[16] NECULOIU D. et al, *AlN on silicon based Surface Acoustic Wave resonators operating at 5 GHz*, El. Letters, vol. **45**, pp. 1196–1197, 2009.

[17] NECULOIU D. et al, *Microwave FBAR Structures Fabricated using Micromachined GaN Membranes*, International Microwave Symposium Digest, IEEE MTT-S, pp. 877–880, 2007.

[18] MÜLLER A., NECULOIU D. et al, *GHz FBAR and SAW resonators manufactured on GaN/Si*, Proceedings of International Semiconductor Conference, CAS 2009, Sinaia, pp. 319–323, 2009.

[19] MÜLLER A., NECULOIU D. et al, *GaN micromachined FBAR structures for microwave applications*, Superlatices & Microstructures, vol. **40**, pp. 426–431, 2006.

[20] MÜLLER A. et al, *6.3 GHz Film Bulk Acoustic Resonator Structures Based on a Gallium Nitride/Silicon Thin Membrane*, IEEE Electron Devices Letters, vol. **30**, no. 8, pp. 799–801, 2009.

[21] CISMARU A., KONSTANTINIDIS G., SZACILOWSKI K., MÜLLER A., STEFANESCU A., STAVRINIDIS A., TSAGARAKI K., KOSTOPULOS T., NECULOIU D., STAVRINIDIS G., BUICULESCU C., KWOLEK P., *Gas and humidity sensors based on high frequency acoustic devices manufactured on GaN/Si*, in *RF MEMS Technologies: Recent Developments, Series in Micro and Nanoengineering*, Editura Academiei Romane, vol. **21**, pp. 263–270, 2012.

[22] *** *CST – Microwave Studio software suite*: `https://www.cst.com/Products/CSTMWS`

[23] GAMEZ-MACHADO A., VALDES-MARTIN D., ASENSIO-LOPEZ A., GISMERO-MENOYO J., *Microstrip-to-stripline planar transitions on LTCC*, IEEE MTT-S International Microwave Workshop Series on Millimeter Wave Integration Technologies (IMWS), pp. 1–4, 15–16 September 2011.

[24] *** *D4.5 – Preliminary LTCC Design Rules, VIA electronic technological requirements.*

[25] *** *DuPont Green Tape*^{TM} *Material System Design and Layout Guidelines.*

[26] MÜLLER A. et al, *GaN-based SAW structures resonating within the 5.4–8.5 GHz frequency range, for high sensitivity temperature sensors*, International Microwave Symposium – IMS 2014, 1–6 June, Tampa, USA, session *TH2F: Sensors and Sensor Systems.*

[27] BUICULESCU V., BECHTOLD F., GIANGU I., MÜLLER A., *LTCC packages optimized for use with SAW and FBAR sensors in environmental parameters monitoring*, Smart System Integration – SSI 2014, pp. 191–197, March 26–27, 2014, Vienna, Austria.

[28] Directive 2002/95/EC of the European Parliament and of the Council of 27 January 2003 on the restriction of the use of certain hazardous substances (*RoHS1*) in electrical and electronic equipment.

[29] Directive 2011/65/EC of the European Parliament and of the Council of 8 June 2011 on the restriction of the use of certain hazardous substances (*RoHS2*) in electrical and electronic equipment.

[30] Regulation (EC) No 1907/2006 of the European Parliament and of the Council of 18 December 2006 concerning the Registration, Evaluation, Authorisation and Restriction of Chemicals (REACH).

[31] GIANGU I., BUICULESCU V., KONSTANTINIDIS G., SZACIŁOWSKI K., STEFANESCU A., BECHTOLD F., PILARCZYK K., STAVRINIDIS A., KWOLEK P., STAVRINIDIS G., MECH J., MÜLLER A., *Acoustic wave sensing devices and their LTCC packaging*, International Semiconductor Conference (CAS) 2014, pp. 147–150, 2014.